Memorias del XVI Congreso Latinoamericano
de Control Automático, CLCA 2014
Octubre 14-17, 2014. Cancún, Quintana Roo, México

Computer implementation of a boundary feedback leak detector and estimator for pipelines I: Transient Model ⋆

Ricardo Lopezlena *

* *Instituto Mexicano del Petróleo (IMP), Investigación en Exploración y Producción. Eje Central Lázaro Cárdenas 152, CP 07730, Ciudad de México, Apdo. Postal 14-805. Tel. +52-9175-7603 (e-mail: rlopezle@imp.mx).*

Abstract: This work is divided in two parts and describes the salient features of a computer system for detection and localization of leaks in pipelines based on a Real-Time Transient Model (RTTM). In this Part I, we discuss our algorithm for pipeline transient simulation, inspired on the port-Hamiltonian formalism for distributed-parameter systems and solved with our ad-hoc *Method of Hamiltonian Characteristics*. Our model includes a Hamiltonian energy function, effects due to terrain topography, multiple leaking points along our finite-dimensional approximation, it admits system interconnections and it is appropriate for a real-time execution. In Part II, such model is used for a closed-loop Luenberger-type boundary feedback estimator of leaks in pipelines, where the leaked flow-rate and leak localization are continuously estimated variables.

Keywords: Modelling, process parameter estimation, pipelines monitoring, pipeline leakage detection, nonlinear systems, distributed-parameter systems.

1. INTRODUCTION

Pipelines contribute to the welfare and development of our societies because they are the *safest*, the *cheapest* and the *most efficient* transportation system for the distribution of water, natural gas, gasoline, LPG, crude oil, and other products, to reach remote and isolated places and populations.

Unfortunately, associated to pipeline operations are also *ruptures*, *product spills*, *leaks* and *clandestine tie-in tappings*. Such safety risks affect our environment, the nearby populations, and also the pipeline facilities, being risks of great concern for all the industrial pipeline operating companies. Therefore improved methods for pipeline *leak detection and localization systems* (LDLS) are relevant for industrial R&D.

In principle, the simplest mass/volume balancing method consists in verifying the steady-state inventory of products transported in a network of pipes. Under nearly steady-state conditions, the pipeline mass/volume balance is calculated as the time-integral of the *balance rate*, defined by the difference of the *flow balance* and the *packing rate*. The balance rate is nearly zero when there is no leak. When a leak is present, the mass unbalance within the network exceeds a threshold and an alarm is displayed, indicating the segment in the network where the unbalance is reported, Whaley et al. (1992). Alternatively, the leak localization can be found from the steady-state *hydraulic-grade line* data, Al-Khomairi (1995). Nevertheless, for long pipelines this approach has a *low detection reliability* because during pipeline transients such as over pressurization (*e.g. water hammer* for incompressible fluids) or *line packing* (due to gas compressibility), these natural transients may lead the steady-state mass/volume balancing method to misleading diagnoses of detected leaks, resulting in false alarms. Clearly, the search for more sophisticated transient modeling methods responds to the need of an increased leak diagnosis reliability. The availability of spatially-distributed data estimated from a *real-time transient model* (RTTM), Nicholas (1987), serves to obtain a better estimation of the line pack/packing rate, improving with this the performance of pipeline product unbalance calculations, since with the RTTM it is possible to discriminate the natural transient behaviors on a network from the real occurrence of leaks, thereby increasing their overall reliability. This approach for leak detection is well known within the civil engineering literature for water applications, see *e.g.* Liou (1990, 1991); Mactaggart and Myers (1996); van Reet and Skogman (1987). Among other methods, leak localization implemented with the RTTM evolved into the *Intersecting hydraulic grade-line method* using two transient models with upstream and downstream boundaries, Al-Khomairi (1995). The availability of a RTTM exceeds the mere objective of surveillance, since such models serve to provide further information of the pipeline, like instrument analysis and the prediction of production rates, justifying their higher maintenance costs.

In this Part I, we discuss our pipeline transient model, inspired on the port-Hamiltonian paradigm for modeling *distributed port-Hamiltonian fluids* (DPHF). The modeling approach of port-Hamiltonian systems is attractive to this work mainly because it results in highly structured models which preserve energy under network interconnection, see *viz.* Pasumarthy and van der Schaft (2004); Hamroun et al. (2007).

The main contribution of this paper is our method of Hamiltonian characteristics which includes effects from terrain topography and multiple leak points along the pipeline.

The paper is organized as follows. In Sect. 2 we provide a brief introduction to the theory of DPHF in order to contextualize the fairly known method of characteristics adapted to this class of systems, presented in Sect. 3 where we also discuss our algorithm for numerical solution. Furthermore, in Sect. 4 we

⋆ This work was supported by Instituto Mexicano del Petróleo. The author is enrolled as Promovendus at the Delft Center for Systems and Control, Delft University of Technology, Delft, The Netherlands.

show some algorithms for the numerical determination of the profiles of a pipeline under the condition of one or multiple leaks along the pipeline. We conclude with some remarks.

2. ENERGY-BASED PIPELINE MODELS

The energy carried by a moving stream of liquid or gas flowing along a pipeline is manifest in several forms:

- *Mechanical kinetic energy:* due to the movement of mass of the fluid at certain velocity along the pipeline.
- *Mechanical potential energy:* due to the weight of the transported fluid at a certain height above sea level.
- *Internal energy:* of the transported fluid due to the internal motion of the molecules, governed mainly by temperature.
- *Work of compression:* The energy supplied by the compressor/pump stations to the gas (liquid) in order to displace the product along the pipeline (*flow work*) overcoming friction forces.
- *Transferred heat energy:* extracted from the fluid due to cooling (heat transfer) effects of the ground around the pipeline, or otherwise, supplied into the fluid due to effects of friction forces.

Thus, while phenomena associated to abrupt, intermittent transitions from kinetic to *elastic energy*/work of compression (*e.g. water hammer*) are more significant for liquids than for gases, phenomena associated to transitions of the internal energy and the work of compression (*e.g. line pack*) are more significant for gases than for liquids.
Most of these mechanical effects can be included in the formulation of the theory of distributed port-Hamiltonian fluid dynamics, discussed briefly in the next section.

2.1 Distributed port-Hamiltonian fluid (DPHF) models

This section is written in an informal style, without mathematical rigor, since it is only intending to collect fundamental facts about one-dimensional DPHF models as an antecedent of our transient model. For a formal presentation see van der Schaft and Maschke (2001, 2002).
We model our pipeline segments with the one-dimensional Euler fluid partial differential equations (PDE) plus the Darcy-Weisbach dissipation term. It consists of the momentum and mass conservation equations:

$$\frac{\partial v}{\partial t} + v\frac{\partial v}{\partial x} + \frac{1}{\rho}\frac{\partial p}{\partial x} + g\frac{\partial z}{\partial x} + \frac{f}{2D}v|v| = 0, \tag{1}$$

$$\frac{\partial \rho}{\partial t} + \frac{\partial (\rho v)}{\partial x} = 0, \tag{2}$$

where $x \in [0, L]$ is the spatial coordinate, t is time, $v(t,x)$ is the fluid velocity, $p(t,x)$ is pressure, $\rho(t,x)$ is density, D is the internal diameter of the pipeline with cross-sectional area $A = \pi D^2/4$, g is the acceleration of gravity, $z(x)$ is the pipeline vertical height (topographic profile w.r.t. sea level) and f is the Darcy-Weisbach dissipation factor. Each segment is contained in a control volume $\forall$ as described in Fig. 1.

Similarly to *Bernoulli Equation* $\frac{v^2}{2} + \frac{p}{\rho} + gz = c, c \in \mathbb{R}$, let us define for each path fluid particle a *specific Hamiltonian* function $h(x,\rho,v,t) = \frac{1}{2}v^2 + u(\rho) + \psi(z)$. Thus, neglecting heat transfer around the pipeline, the *total energy* in $\forall$ transported by the pipeline can be described by (see *e.g.* Lopezlena and Scherpen (2004)) the Hamiltonian functional $\mathcal{H}(\rho,v,t) \stackrel{\text{def}}{=} \int_{\forall} \rho h(x,\rho,v,t)\, d\forall$ given by

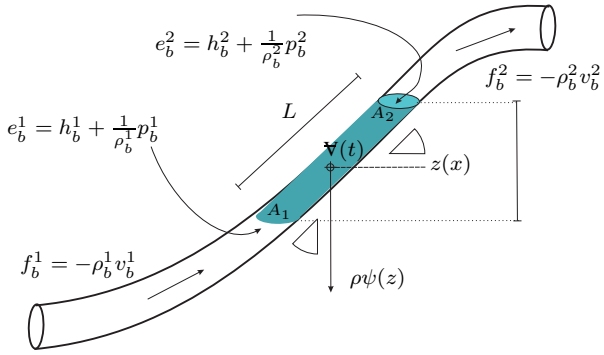

Fig. 1. Free-body diagram for a DPHF model with boundaries.

$$\mathcal{H}(\rho,v,t) = \int_{\forall} \left\{ \frac{1}{2}\rho v^2 + \rho u(\rho) + \rho\psi(z(x)) \right\} d\forall. \tag{3}$$

Each term within keys is a *density of energy* associated to the traveling stream along the pipeline. While $\frac{1}{2}\rho v^2$ accounts for the kinetic energy, $\rho u(\rho)$ accounts for the internal energy and the term $\rho\psi(z)$ accounts for the (gravitational) potential energy. The work of compression and enthalpy crop up later.
Eqs. (1)-(2) can be described by a DPHF model expressed by:

$$\begin{bmatrix} \partial_t \rho \\ \partial_t v \end{bmatrix} = \begin{bmatrix} 0 & -d \\ -d & -R_d \end{bmatrix} \begin{bmatrix} \delta_\rho \mathcal{H} \\ \delta_v \mathcal{H} \end{bmatrix}, \tag{4}$$

where ∂ denotes partial derivatives, δ *functional derivatives*, d is a *differential operator* and $R_d \stackrel{\text{def}}{=} \frac{f}{2\rho D}|v|$. We can verify that indeed this is a distributed port-Hamiltonian representation of Eqs. (1)-(2) as follows (for the use of functional derivatives see e.g. Morrison (1998)). Since the functional derivatives of the Hamiltonian functional (3) are given by

$$\delta_\rho \mathcal{H} = \frac{1}{2}v^2 + \frac{\partial}{\partial \rho}\left(\rho u(\rho)\right) + \psi(z), \tag{5}$$

$$\delta_v \mathcal{H} = \rho v, \tag{6}$$

and since $\frac{\partial}{\partial \rho}\left(\rho u(\rho)\right) = u(\rho) + \rho\frac{\partial}{\partial \rho}\left(u(\rho)\right)$, using the following thermodynamic identity, see *e.g.* Callen (1985),

$$p(x,t) = \rho^2 \left(\frac{\partial u(x,\rho)}{\partial \rho} \right)_s, \tag{7}$$

(where the subscript s stands for *isentropic conditions*) we may rewrite Eq. (5) as

$$\delta_\rho \mathcal{H} = \frac{1}{2}v^2 + \overbrace{u(\rho) + \frac{1}{\rho}p(t,x)}^{\text{Specific enthalpy } \eta} + \psi(z), \tag{8}$$

where the *specific enthalpy* $\eta = u + p\forall = u + p/\rho$, (*i.e.* the sum of the specific internal energy plus the work of compression) emerges naturally from the equations. If the *gravitational potential* is defined as $\psi(z) = gz(x)$, see *e.g.* Batchelor (1967), with the dissipation term R_d, we get

$$\begin{aligned} d(\delta_\rho \mathcal{H}) &= v\frac{\partial v}{\partial x} + \frac{\partial u(\rho)}{\partial \rho}\frac{\partial \rho}{\partial x} + \frac{1}{\rho}\frac{\partial p}{\partial x} - \frac{p}{\rho^2}\frac{\partial \rho}{\partial x} + \frac{\partial}{\partial x}\psi(z), \\ &= v\frac{\partial v}{\partial x} + \frac{1}{\rho}\frac{\partial p}{\partial x} + \left(\frac{\partial u(\rho)}{\partial \rho} - \frac{p}{\rho^2} \right)\frac{\partial \rho}{\partial x} + g\frac{\partial z}{\partial x}, \\ &= v\frac{\partial v}{\partial x} + \frac{1}{\rho}\frac{\partial p}{\partial x} + g\frac{\partial z}{\partial x}, \end{aligned} \tag{9}$$

where the identity (7) was newly used. Now, since

$$d(\delta_v \mathcal{H}) = \frac{\partial (\rho v)}{\partial x} = \rho\frac{\partial v}{\partial x} + v\frac{\partial \rho}{\partial x}, \tag{10}$$

then after substitution of (9) and (10) in Eqs. (4) we obtain

$$\frac{\partial \rho}{\partial t} = -\frac{\partial(\rho v)}{\partial x},$$
$$\frac{\partial v}{\partial t} = -v\frac{\partial v}{\partial x} - \frac{1}{\rho}\frac{\partial p}{\partial x} - g\frac{\partial z}{\partial x} - \frac{f}{2D}v|v|,$$

which are Eqs. (1)-(2), confirming the assertion that Eq. (4) provides an equivalent representation to Eqs. (1)-(2).
In the port-Hamiltonian formalism, the exchange of energy through the pipeline boundaries are expressed by:

$$\begin{bmatrix} e_b \\ f_b \end{bmatrix} = \begin{bmatrix} 1 & 0 \\ 0 & -1 \end{bmatrix} \begin{bmatrix} \delta_\rho \mathcal{H}|_{\partial \forall} \\ \delta_v \mathcal{H}|_{\partial \forall} \end{bmatrix}. \tag{11}$$

We may be convinced of this latter assertion by the following arguments. The boundaries (11) can be expressed by

$$e_b = \delta_\rho \mathcal{H}|_{\partial \forall} = h_b + \frac{1}{\rho_b} p_b = h_b + \forall_b p_b, \tag{12}$$
$$f_b = -\delta_v \mathcal{H}|_{\partial \forall} = -\rho_b v_b, \tag{13}$$

where $h_b = \frac{1}{2}v_b^2 + u_b(\rho_b) + \psi_b$ is the *specific Hamiltonian at the boundary* and $p_b \forall_b$ is the specific contribution to the *flow work* through the port. If we perform a total energy balance with the Hamiltonian functional $\mathcal{H}(\rho, v, t)$, Eq. (3), contained in the control volume $\forall$, we obtain naturally

$$\frac{d}{dt}\mathcal{H}(\rho, v, t) = \frac{\delta \mathcal{H}}{\delta \rho}\frac{\partial \rho}{\partial t} + \frac{\delta \mathcal{H}}{\delta v}\frac{\partial v}{\partial t} = \int_{\partial \forall} (f_b\, e_b)\, d\partial\forall, \tag{14}$$

thus, the transferred energy through the port is given by

$$\int_{\partial \forall} (f_b\, e_b)\, d\partial\forall = -\int_A (h + \frac{p}{\rho})\rho \mathbf{v} dA, \tag{15}$$

confirming that the total energy is transferred through the boundary, including the flow work. Since there are two boundaries A_1 and A_2 located at both ends of the pipeline in Fig. 1, then

$$\int_{\partial \forall} (f_b\, e_b)\, d\partial\forall = \int_{A_1} (h + \frac{p}{\rho})\rho \mathbf{v} dA - \int_{A_2} (h + \frac{p}{\rho})\rho \mathbf{v} dA.$$

The relevance of the latter is that if two systems of this class are interconnected by their ports, the total energy is preserved. See Pasumarthy and van der Schaft (2004) for an extended discussion on port interconnections.

Remark 2.1. When $\partial_x \psi(z) = 0$ and the Darcy-Weisbach factor is null, then Eqs. (4)-(11) with the Hamiltonian functional (3) are the one-dimensional version of the Euler Equations expressed in the general distributed port-Hamiltonian form introduced by van der Schaft and Maschke (2001, 2002).

3. THE CHARACTERISTICS OF HAMILTONIAN SYSTEMS

Assume that the set solution of a first-order partial differential equation, expressed as $\xi \cdot \nabla u = 0$, lies in a manifold M. The *characteristic curves* are integral trajectories of tangent vector fields $\xi \in TM$ solution of such first-order equation, normal to ∇u. If a first-order PDE on an n-dimensional space is transformed into the *characteristic coordinates*, in such coordinates the PDE is transformed into a system of n-ordinary differential equations (ODE). In practical terms, this means that such PDE can be reduced into a set of ODE, which can be solved on the intersections of the integrated characteristic curves, this is called the *method of characteristics* (MOC).
There is a very close relationship between the *characteristic trajectories* of the Hamilton-Jacobi equation and the solution of its associated Hamiltonian system, since after all a Hamiltonian system can be expressed as $\xi \cdot \nabla H = 0, \xi \in TM, \nabla H \in T^*M$. Consider a closed, finite-dimensional Hamiltonian system with principal generating function $S(q_i, t)$ such that it satisfies the Hamilton-Jacobi equation $\frac{\partial S}{\partial t} + H(q, p) = 0$ with Hamiltonian function $H(q, p)$ where $q = (q_1, \ldots, q_n)$, $p = (p_1, \ldots, p_n)$, $p_i = \frac{\partial S}{\partial q_i}$. Then it is known (for a proof see Debnath (1997); Sneddon (1957)) that their characteristic equations are equivalent to the Hamilton equations of motion.

$$\frac{dq_i}{dt} = \frac{\partial H}{\partial p_i}, \quad \frac{dp_i}{dt} = -\frac{\partial H}{\partial q_i}, \quad i = 1, 2, \ldots, n$$

Using similar arguments for port-Hamiltonian systems, it can be asserted that the characteristics of the local Hamiltonian function $\mathcal{H}_i(\rho, v, t)$, $i = 1, \ldots, n_s$ is given by the trajectories $(\rho_i(t), v_i(t))$ solution of the system of differential equations associated to the port-Hamiltonian representation (4)-(11) of the fluid equations (1)-(2).
It should be observed though, that time-integration for Hamiltonian systems is a delicate stage, since it should preserve their *symplectic-structure*, see *e.g.* Hairer et al. (2002).

3.1 The method of Hamiltonian characteristics (MOHC)

Based on the previous section, we present a numerical algorithm to solve the fluid system of PDEs given by Eqs. (1)-(2), by transforming them into ODEs (in Prop. 3.1) and then by integrating them along its characteristic curves (in Prop. 3.2).

Proposition 3.1. (Hamiltonian Characteristics). Assume isentropic conditions and the *speed of sound* a_s s.t. $a_s >> v$. The characteristics of the PDE defined in Eqs. (1)-(2) are the set solution of the following ODEs:

$$C^+ \begin{cases} \dfrac{dv}{dt} + \dfrac{a_s}{\rho}\dfrac{d\rho}{dt} + \dfrac{g}{2(a_s + v)}\dfrac{dz}{dt} + \dfrac{f}{4D}v|v| = 0, \\ \dfrac{dx}{dt} = v + a_s, \end{cases} \tag{16}$$

$$C^- \begin{cases} \dfrac{dv}{dt} - \dfrac{a_s}{\rho}\dfrac{d\rho}{dt} - \dfrac{g}{2(a_s - v)}\dfrac{dz}{dt} + \dfrac{f}{4D}v|v| = 0, \\ \dfrac{dx}{dt} = v - a_s. \end{cases} \tag{17}$$

(See Appendix A for the proof).
A relationship between $p(t, x)$ and $\rho(t, x)$ is required:

Remark 3.1. Under isentropic conditions, density and pressure are related in differential form, White (1991), by:

$$dp = \left(\frac{\partial p}{\partial \rho}\right)_s d\rho = a_s^2\, d\rho, \tag{18}$$

where a_s is defined by $a_s^2 \overset{\text{def}}{=} (\partial p/\partial \rho)_s$. A local relationship between $p(t, x)$ and $\rho(t, x)$, useful for computations, can be derived from Eq. (18) after integration around a reference point $(p_{\text{ref}}, \rho_{\text{ref}})$, yielding:

$$\rho = \frac{k + p}{a_s^2} \quad \Longleftrightarrow \quad p = \rho a_s^2 - k, \tag{19}$$

where $k \overset{\text{def}}{=} a_s^2 \rho_{\text{ref}} - p_{\text{ref}}$, see also Aamo et al. (2006).

Alternatively, the *Real Gas Law* $p = \rho Z R T$ (where Z is the *compressibility factor*, R the *gas constant* and T *temperature*) could be used for ducts transporting fluids in gas phase.

Proposition 3.2. (MOC and MOHC). Let us assume $a_s >> v$, isentropic conditions and initial given values of nodal coordinates $(\rho_P^i, p_P^i, v_P^i)_k$ for $i = 0, 1, \ldots, n_n - 1$ (where $n_n \in \mathbb{Z}^+$, $n_n = L/\Delta x + 1$ is the number of nodes) along the characteristics (16)-(17) in the grid defined in Fig. 2. The solution of Eqs.

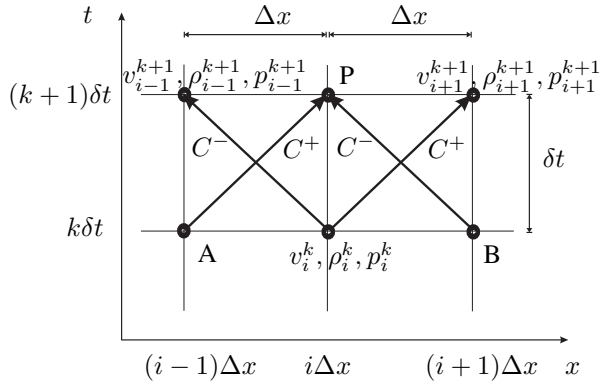

Fig. 2. Nodal grid (v, ρ, p) of Hamiltonian characteristics.

(1)-(2) for every sampled time $\delta t \stackrel{\text{def}}{=} \Delta x/a_s$, given by the points P_{k+1} along the characteristics (16)-(17) where $t = (k+1)\delta t$, can be obtained from the following three assertions:

(1) The points $P_{k+1} \stackrel{\text{def}}{=} (\rho_P^i, v_P^i)_{k+1}$, $i = 0, 1, \ldots, n_n - 1$ in the grid can be found from the linear system of eqs.:

$$\begin{bmatrix} a^i & b^i \\ c^i & d^i \end{bmatrix}_k \begin{bmatrix} v_P^i \\ \ln|\rho_P^i| \end{bmatrix}_{k+1} = \begin{bmatrix} e^i \\ f^i \end{bmatrix}_k \tag{20}$$

for $i = 0, \ldots, n_n - 1$, where

$$a^i \stackrel{\text{def}}{=} 1 + |v_A|\, \delta t\, f/4D, \tag{21}$$

$$b^i \stackrel{\text{def}}{=} a_s, \tag{22}$$

$$c^i \stackrel{\text{def}}{=} 1 + |v_B|\, \delta t\, f/4D, \tag{23}$$

$$d^i \stackrel{\text{def}}{=} -a_s, \tag{24}$$

$$e^i \stackrel{\text{def}}{=} v_A + a_s \ln|\rho_A| - \frac{g(z_P - z_A)}{2(a_s + v_A)}, \tag{25}$$

$$f^i \stackrel{\text{def}}{=} v_B - a_s \ln|\rho_B| + \frac{g(z_P - z_B)}{2(a_s - v_B)}. \tag{26}$$

(2) The points $P_{k+1} \stackrel{\text{def}}{=} (p_P^i, v_P^i)_{k+1}$, $i = 0, 1, \ldots, n_n - 1$ in the grid can be found from the linear system of eqs.:

$$\begin{bmatrix} a^i & g^i \\ c^i & h^i \end{bmatrix}_k \begin{bmatrix} v_P^i \\ p_P^j \end{bmatrix}_{k+1} = \begin{bmatrix} m^i \\ n^i \end{bmatrix}_k \tag{27}$$

for $i = 0, \ldots, n_n - 1$, where a^i and c^i are defined by Eqs. (21)-(22) and the remaining variables as follows:

$$g^i = 1/(\rho_A a_s), \tag{28}$$

$$h^i = -1/(\rho_B a_s), \tag{29}$$

$$m^i = v_A + \frac{p_A}{\rho_A a_s} - \frac{g(z_P - z_A)}{2(a_s + v_A)}, \tag{30}$$

$$n^i = v_B - \frac{p_B}{\rho_B a_s} + \frac{g(z_P - z_B)}{2(a_s - v_B)}. \tag{31}$$

(3) The simultaneous solution for $P_{k+1} \stackrel{\text{def}}{=} (\rho_P^i, p_P^i, v_P^i)_{k+1}$, $i = 0, \ldots, n_n - 1$ in the grid can be found from the linear system of eqs.:

$$\begin{bmatrix} 2a^i & b^i & g^i \\ c^i & d^i & 0 \\ c^i & 0 & h^i \end{bmatrix}_k \begin{bmatrix} v_P^i \\ \ln|\rho_P^i| \\ p_P^j \end{bmatrix}_{k+1} = \begin{bmatrix} e^i + m^i \\ f^i \\ n^i \end{bmatrix}_k \tag{32}$$

with variables defined as in Eqs. (21)-(26), (28)-(31).

(See Appendix B for the proof.)

Remark 3.2. The Hamiltonian function (3) is given by

$$\mathcal{H}(\rho, v, t) = \sum_{i=0}^{n_n - 1} \left\{ \frac{1}{2}\rho_i (v_i)^2 + \rho_i u(\rho_i) + \rho_i g z_i \right\} A_i \Delta x,$$

and the boundaries of the DPHFS defined in Eqs. (12)-(13) can be constructed from the boundary points $P_k^0 \stackrel{\text{def}}{=} (\rho_P^0, p_P^0, v_P^0)_k$ and $P_k^{n_n-1} \stackrel{\text{def}}{=} (\rho_P^{n_n-1}, p_P^{n_n-1}, v_P^{n_n-1})_k$.
Moreover, based on the input variables at their boundaries, several pipeline model structures can be constructed.

Example 3.1. Consider a pipeline model as in Prop. 3.2 assertion (1) with 3 nodes ($n_n = 3$) and boundary inputs $(v_u, \rho_d) = (v_0, \rho_2)$. Then we obtain a system of equations:

$$\begin{bmatrix} d^0 & 0 & 0 & 0 \\ 0 & a^1 & b^1 & 0 \\ 0 & c^1 & d^1 & 0 \\ 0 & 0 & 0 & a^2 \end{bmatrix} \begin{bmatrix} \ln|\rho_0^{k+1}| \\ v_1^{k+1} \\ \ln|\rho_1^{k+1}| \\ v_2^{k+1} \end{bmatrix} = \begin{bmatrix} f^0 - c^0 v_0^{k+1} \\ e^1 \\ f^1 \\ e^2 - b^2 \ln|\rho_2^{k+1}| \end{bmatrix} \tag{33}$$

whose solution is evidently given by

$$\begin{cases} \ln|\rho_0^{k+1}| = (f^0 - c^0 v_0^{k+1})/d^0, & i = 0 \\ v_i^{k+1} = \dfrac{e^i d^i - b^i f^i}{a^i d^i - b^i c^i}, & i = 1, \ldots, n_n - 2 \\ \ln|\rho_i^{k+1}| = \dfrac{a^i f^i - c^i e^i}{a^i d^i - b^i c^i}, & i = 1, \ldots, n_n - 2 \\ v_2^{k+1} = (e^2 - b^2 \ln|\rho_2^{k+1}|)/a^2, & i = n_n - 1 \end{cases}$$

and pressure p_i for $i = 0, \ldots, n_n - 1$ is found from Rem. 3.1. Based on Proposition 3.2, other models with different boundaries can be constructed from assertions (1), (2) and (3).

4. MODEL WITH MULTIPLE LEAKING POINTS

In preparation to Part II, assume that there is a leak with localization x_ℓ and flow rate magnitude $w_\ell \stackrel{\text{def}}{=} \rho^\ell \tilde{v}^\ell A^\ell = \rho v^\ell A$ where $v^\ell \stackrel{\text{def}}{=} \frac{\rho^\ell A^\ell}{\rho A} \tilde{v}^\ell$. Such leak can be modeled as two pipeline segments with an intermediate port whose boundary conditions define the leak, see Fig. 3. We assume x_ℓ coincides with some

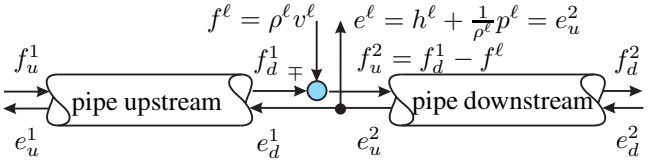

Fig. 3. Boundary variables for a leaking port inserted along a DPHFS model.

j-node, therefore, there are $n_n - 1$ different possible localizations. In order to include a leaking port into the computational formulation of the Hamiltonian Characteristics method, let $P_{k+1}^j \stackrel{\text{def}}{=} (\rho_P^j, v_P^j)_{k+1}$. In such point Eq. (20) would model the node equations if there where no leaks. In the presence of a leak, there is a new boundary for the upstream segment such that $e_d^1 = e_u^2$ and $f_u^2 = f_d^1 - f^\ell$ at the common j-node joining both segments. Let v_j^ℓ be the velocity of leaked flow rate $w_\ell = \rho v_j^\ell A$, then $v_j^k \stackrel{\text{def}}{=} v_j^k - v_j^\ell$. After substitution and reordering in Eq. (20) we obtain the desired system of eqs.

Example 4.1. Consider the system interconnection of two DPHF segment models as in Fig. 3, where each (v_u, ρ_d)-model has the same structure (33) of Example 3.1 and a common boundary with a leak located in the 2-node in the nodal grid of

Fig. 2, for $i = 0 \ldots 4$. Then the following system of equations is obtained:

$$\begin{bmatrix} d^0 & 0 & 0 & 0 & 0 & 0 & 0 & 0 \\ 0 & a^1 & b^1 & 0 & 0 & 0 & 0 & 0 \\ 0 & c^1 & d^1 & 0 & 0 & 0 & 0 & 0 \\ 0 & 0 & 0 & a^2 & b^2 & 0 & 0 & 0 \\ 0 & 0 & 0 & c^2 & d^2 & 0 & 0 & 0 \\ 0 & 0 & 0 & 0 & 0 & a^3 & b^3 & 0 \\ 0 & 0 & 0 & 0 & 0 & c^3 & d^3 & 0 \\ 0 & 0 & 0 & 0 & 0 & 0 & 0 & a^4 \end{bmatrix} \begin{bmatrix} \ln|\rho_0^{k+1}| \\ v_1^{k+1} \\ \ln|\rho_1^{k+1}| \\ v_2^{k+1} \\ \ln|\rho_2^{k+1}| \\ v_3^{k+1} \\ \ln|\rho_3^{k+1}| \\ v_4^{k+1} \end{bmatrix} = \begin{bmatrix} f^0 - c^0 v_0^{k+1} \\ e^1 \\ f^1 \\ e^2 \\ f^2 + c^2 v_2^\ell \\ e^3 \\ f^3 \\ e^4 - b^4 p_4^{k+1} \end{bmatrix}$$

This constructive procedure to include the leaking port into the system of Eqs. (20) that solve the fluid equations, can be repeated for the block matrices (27) and (32) from Prop. 3.2. More formally, we collect these findings in the following

Proposition 4.1. Let a leaking port be located at the point P_k^j in the j-node with leaked (mass) flow rate $w_\ell = \rho_j v_j^\ell A$. Then

(1) Let $P_{k+1}^j \stackrel{\text{def}}{=} (\rho_P^j, v_P^j)_{k+1}$, then the block matrix equation for $i = 0, \ldots, n_n - 1$ is given by

$$\begin{bmatrix} a^i & b^i \\ c^i & d^i \end{bmatrix}_k \begin{bmatrix} v_P^i \\ \ln|\rho_P^i| \end{bmatrix}_{k+1} = \begin{bmatrix} e^i \\ f^i + c^j v_j^\ell \end{bmatrix}_k . \quad (34)$$

(2) Let $P_{k+1}^j \stackrel{\text{def}}{=} (p_P^j, v_P^j)_{k+1}$ then the block matrix equation is given by

$$\begin{bmatrix} a^i & g^i \\ c^i & h^i \end{bmatrix}_k \begin{bmatrix} v_P^i \\ p_P^j \end{bmatrix}_{k+1} = \begin{bmatrix} m^i \\ n^i + c^j v_j^\ell \end{bmatrix}_k . \quad (35)$$

(3) Let $P_{k+1}^j \stackrel{\text{def}}{=} (\rho_P^i, p_P^j, v_P^j)_{k+1}$ then the block matrix equation is given by

$$\begin{bmatrix} 2a^i & b^i & g^i \\ c^i & d^i & 0 \\ c^i & 0 & h^i \end{bmatrix}_k \begin{bmatrix} v_P^i \\ \ln|\rho_P^i| \\ p_P^j \end{bmatrix}_{k+1} = \begin{bmatrix} e^i + m^i \\ f^i + c^j v_j^\ell \\ n^i + c^j v_j^\ell \end{bmatrix}_k \quad (36)$$

As an evident consequence of Prop. 4.1, we may insert leaking ports in $n_n - 1$ localizations.

Example 4.2. (Flute-pipeline model). Consider again Example 4.1, under a multi-leak condition, *i.e.* for each i-node there is a leak, which we express by the vector $v^\ell = \begin{bmatrix} v_0^\ell & v_1^\ell & v_2^\ell & v_3^\ell \end{bmatrix}^T$. Then we obtain a system of equations:

$$\begin{bmatrix} d^0 & 0 & 0 & 0 & 0 & 0 & 0 & 0 \\ 0 & a^1 & b^1 & 0 & 0 & 0 & 0 & 0 \\ 0 & c^1 & d^1 & 0 & 0 & 0 & 0 & 0 \\ 0 & 0 & 0 & a^2 & b^2 & 0 & 0 & 0 \\ 0 & 0 & 0 & c^2 & d^2 & 0 & 0 & 0 \\ 0 & 0 & 0 & 0 & 0 & a^3 & b^3 & 0 \\ 0 & 0 & 0 & 0 & 0 & c^3 & d^3 & 0 \\ 0 & 0 & 0 & 0 & 0 & 0 & 0 & a^4 \end{bmatrix} \begin{bmatrix} \ln|\rho_0^{k+1}| \\ v_1^{k+1} \\ \ln|\rho_1^{k+1}| \\ v_2^{k+1} \\ \ln|\rho_2^{k+1}| \\ v_3^{k+1} \\ \ln|\rho_3^{k+1}| \\ v_4^{k+1} \end{bmatrix} = \begin{bmatrix} \zeta^0 + c^0 v_0^\ell \\ e^1 \\ f^1 + c^1 v_1^\ell \\ e^2 \\ f^2 + c^2 v_2^\ell \\ e^3 \\ f^3 + c^3 v_3^\ell \\ \zeta^4 \end{bmatrix},$$

where $\zeta^0 \stackrel{\text{def}}{=} f^0 - c^0 v_0^{k+1}$ and $\zeta^4 = e^4 - b^4 p_4^{k+1}$.

5. CONCLUDING REMARKS

Acceptedly, a multi-leaks pipeline model based on a centered-differences scheme was introduced earlier in Billmann and Isermann (1987). Simulations of the isentropic multi-leaks transient model presented in this paper are deferred to Part II, where we test the implemented leak localization algorithm. A more accurate model would include the pipeline material elasticity, the influence on the fluid temperature by heat transfer through the boundaries of the pipeline and presence of two-phase flow.

REFERENCES

Aamo, O., Salvesen, J., and Foss, B.A. (2006). "Observer design using boundary injections for Pipeline Monitoring and Leak Detection". In *Int. Symp. on Adv. Control of Chemical Processes ADCHEM 2006*. Gramado, Brazil, April 2-5.

Al-Khomairi, A.M. (1995). *Improving leak detectability in long liquids pipelines*. Ph. D. Thesis, Colorado State Univ.

Batchelor, G.K. (1967). *An introduction to fluid dynamics*. Math. Library. Cambridge Univ., USA.

Billmann, L. and Isermann, R. (1987). "Leak Detection Methods for Pipelines". *Automatica*, 23(3), 381–385.

Callen, H.B. (1985). *Thermodynamics and an introduction to Thermostatistics*. Wiley, USA, 2^{nd} edition.

Debnath, L. (1997). *Nonlinear Partial Differential Equations for scientist and engineers*. Birkhaüser, Boston, USA.

Hairer, E., Lubich, C., and Wanner, G. (2002). *Geometric Numerical Integration: Structure Preserving Algorithms for ordinary differential equations*. Computational Math. 31. Springer Verlag, Berlin, Germany.

Hamroun, B., Lefevre, L., and Mendes, E. (2007). "Port-based Modelling for Open Channel Irrigation Systems". In *Proc. 2nd IASME/WSEAS Int. Conf. Water Res., Hydr. & Hydrol.* Portoroz, Slovenia, May 15-17.

Liou, C. (1990). "Pipeline leak detection and location". In *Proc. Int. ASCE Conf. Pipeline Design and Installation*, 255–269. Las Vegas, Nevada USA, March 25-27.

Liou, J. (1991). "Leak detection and location by transient flow simulations". In *Proc. of The API Pipeline Conf.*, 268–281. Dallas, Texas USA, April 23-24.

Lopezlena, R. and Scherpen, J. (2004). "On Distributed Port-Hamiltonian Process Systems". In *Proc.* 6^{th} *IFAC Symp. in Nonlin. Cont. Syst. NOLCOS'2004*. Stuttgart, Germany.

Mactaggart, R. and Myers, R. (1996). "PC Based Leak Detection". In *Proc.* 1^{st} *Int. Pipeline Conf. (IPC'96), ASME Vol 2*, 1101–1108. Calgary, Canada, June 9-13.

Morrison, P.J. (1998). "Hamiltonian description of the ideal fluid". *Reviews of Modern Physics*, 70(2), 467–521.

Nicholas, R. (1987). "Leak detection by model compensated volume balance". In *ASME Pipeline Engineering Symp.-ETCE 1987*, 13–20. Dallas, Texas USA, February 15-18.

Pasumarthy, R. and van der Schaft, A. (2004). "On interconnections of infinite dimensional port-Hamiltonian systems". In *Proc.* 16^{th} *Int. Symp. on Math. Th. of Net. and Syst. (MTNS2004)*. Leuven, Belgium.

Sneddon, I. (1957). *Elements of partial differential equations*. Mathematics series. McGraw-hill, Singapore.

van der Schaft, A.J. and Maschke, B.M. (2001). "Fluid dynamical systems as Hamiltonian boundary control systems". In *Proc. Conf. on Dec. and Cont.*, 4497–4502. Orlando Fl.

van der Schaft, A.J. and Maschke, B.M. (2002). "Hamiltonian formulation of distributed -parameter systems with boundary energy flow". *J. of Geometry and Physics*, 42, 166–194.

van Reet, J. and Skogman, K. (1987). "The effect of Measurement uncertainty on Real Time pipeline modeling applications". In *ASME Pipeline Engineering Symp.-ETCE 1987*, 29–33. Dallas, Texas USA, February 15-18.

Whaley, R., Nicholas, R., and van Reet, J. (1992). "Tutorial on Software Based Leak Detection Techniques". Pipeline Simulation Interest Group, October, pp 1-19.

White, F.M. (1991). *Viscous Fluid Flow*. McGraw-Hill, Singapore, 2^{nd} edition.

Appendix A. PROOF OF PROPOSITION 3.1

Proof. Let us define a multiplier λ:

$$\lambda\left(\frac{\partial v}{\partial t}+v\frac{\partial v}{\partial x}+\frac{1}{\rho}\frac{\partial p}{\partial x}+g\frac{\partial z}{\partial x}+\frac{f}{2D}v|v|\right) +\frac{\partial \rho}{\partial t}+\rho\frac{\partial v}{\partial x}+v\frac{\partial \rho}{\partial x}=0,$$

and reorder it as

$$\lambda\frac{\partial v}{\partial t}+\rho\frac{\partial v}{\partial x}+\lambda v\frac{\partial v}{\partial x}+\frac{\lambda}{\rho}\frac{\partial p}{\partial x}+\frac{\partial \rho}{\partial t} +v\frac{\partial \rho}{\partial x}+\lambda g\frac{\partial z}{\partial x}+\lambda\frac{f}{2D}v|v|=0.$$

For isentropic conditions, after Eq. (18) we get

$$\underbrace{\lambda\frac{\partial v}{\partial t}+(\rho+\lambda v)\frac{\partial v}{\partial x}}_{2\lambda dv/dt}+\underbrace{\frac{\partial \rho}{\partial t}+\left(\frac{\lambda}{\rho}a_s^2+v\right)\frac{\partial \rho}{\partial x}}_{2d\rho/dt} +\lambda g\frac{\partial z}{\partial x}+\lambda\frac{f}{2D}v|v|=0. \quad \text{(A.1)}$$

Now, with the purpose of determining total derivatives, we observe that

$$\lambda\frac{\partial v}{\partial t}+\overbrace{(\rho+\lambda v)}^{\lambda dx/dt}\frac{\partial v}{\partial x}\overset{\text{def}}{=}2\lambda\frac{dv}{dt}, \quad \text{(A.2)}$$

only if $\frac{\rho}{\lambda}+v=\frac{dx}{dt}$. On the other side, notice that

$$\frac{\partial \rho}{\partial t}+\overbrace{\left(\frac{\lambda}{\rho}a_s^2+v\right)}^{dx/dt}\frac{\partial \rho}{\partial x}\overset{\text{def}}{=}2\frac{d\rho}{dt}, \quad \text{(A.3)}$$

only if it is verified that $\frac{\lambda}{\rho}a_s^2+v=\frac{dx}{dt}$, thus by equating $\frac{\rho}{\lambda}+v=\frac{\lambda}{\rho}a_s^2+v$, yields $\lambda=\pm\rho/a_s$ and thus the characteristics are given by

$$\begin{cases} C^+: & \dfrac{dx}{dt}=v+a_s, \\ C^-: & \dfrac{dx}{dt}=v-a_s. \end{cases} \quad \text{(A.4)}$$

After substitution of Eqs. (A.2)-(A.3) in Eq. (A.1) we get

$$2\lambda\frac{dv}{dt}+2\frac{d\rho}{dt}+\lambda g\frac{\partial z}{\partial x}+\lambda\frac{f}{2D}v|v|=0. \quad \text{(A.5)}$$

Then, after (A.4), there are two options:

- For $\lambda=+\rho/a_s$ in Eq. (A.5), since $\frac{\partial z}{\partial t}=\frac{\partial z}{\partial x}\frac{\partial x}{\partial t}=(a_s+v)\frac{\partial z}{\partial x}$ and multiplying by $\frac{a_s}{2\rho}$, yields:

$$C^+: \quad \frac{dv}{dt}+\frac{a_s}{\rho}\frac{d\rho}{dt}+\frac{g}{2(a_s+v)}\frac{\partial z}{\partial t}+\frac{f}{4D}v|v|=0,$$

- For $\lambda=-\rho/a_s$ in Eq. (A.5), since $\frac{\partial z}{\partial t}=\frac{\partial z}{\partial x}\frac{\partial x}{\partial t}=-(a_s-v)\frac{\partial z}{\partial x}$ and multiplying by $\frac{-a_s}{2\rho}$, yields:

$$C^-: \quad \frac{dv}{dt}-\frac{a_s}{\rho}\frac{d\rho}{dt}-\frac{g}{2(a_s-v)}\frac{\partial z}{\partial t}+\frac{f}{4D}v|v|=0,$$

implying that the characteristics C^+ and C^- are determined by the solution of the (ordinary-differential) Eqs. (16)-(17) whenever Eqs. (A.4) are satisfied.

Appendix B. PROOF OF PROPOSITION 3.2

Proof. 1) Let us rewrite Eqs. (16)-(17) in differential form to obtain

$$C^+: \quad dv+\frac{a_s}{\rho}d\rho+\frac{g}{2(a_s+v)}dz+\frac{f}{4D}v|v|dt=0,$$
$$C^-: \quad dv-\frac{a_s}{\rho}d\rho-\frac{g}{2(a_s-v)}dz+\frac{f}{4D}v|v|dt=0.$$

In order to proceed with the integration along C^+ and C^-, consider now Figure 2, and obtain for C^+ :

$$v_P-v_A+a_s\int_A^P\frac{d\rho}{\rho}+\frac{g}{2(a_s+v_A)}\int_A^P dz +\int_A^P\frac{f}{4D}v|v|\,dt=0,\ \text{s.t.}\quad x_P-x_A=\int_A^P(v+a_s)\,dt,$$

and for C^- :

$$v_P-v_B-a_s\int_B^P\frac{d\rho}{\rho}-\frac{g}{2(a_s-v_B)}\int_B^P dz +\int_B^P\frac{f}{4D}v|v|\,dt=0,\ \text{s.t.}\quad x_P-x_B=\int_B^P(v-a_s)\,dt.$$

Now, since $\int\frac{d\rho}{\rho}=\ln|\rho|$, we obtain the equations, for C^+

$$v_P-v_A+a_s(\ln|\rho_P|-\ln|\rho_A|)+\frac{g(z_P-z_A)}{2(a_s+v_A)}+v_P\frac{f}{4D}|v_A|\,\delta t=0, \quad \text{(B.1)}$$

whenever $\frac{\delta t}{\Delta x}=\frac{1}{v+a_s}$. Using the same identity for C^-:

$$v_P-v_B-a_s(\ln|\rho_P|-\ln|\rho_B|)-\frac{g(z_P-z_B)}{2(a_s-v_B)}+v_P\frac{f}{4D}|v_B|\,\delta t=0, \quad \text{(B.2)}$$

whenever $\frac{\delta t}{\Delta x}=\frac{1}{v-a_s}$. Since the point $P_{k+1}\overset{\text{def}}{=}(\rho_P^i,v_P^i)_{k+1}$ in the grid must satisfy equations (B.1)-(B.2) simultaneously, consider the definition of variables in Eqs. (21)-(26), then Eqs. (B.1)-(B.2) can be reformulated to take the form of Eq. (20), a system of linear equations. The extension for $i=0,\ldots,n_n-1$ follows immediately.

2) Using Eq. (18), rewrite Eq. (2) to obtain

$$\frac{1}{\rho}\frac{\partial p}{\partial t}+\frac{v}{\rho}\frac{\partial p}{\partial x}+a_s^2\frac{\partial v}{\partial x}=0.$$

Repeat the procedure in the proof of Prop. 3.1 in terms of variables (p,v), using $\lambda=\pm a_s$. The resulting characteristics are equivalent to Eqs. (16)-(17), since by Eq. (18), $\frac{a_s}{\rho}\frac{d\rho}{dt}=\frac{1}{\rho a_s}\frac{dP}{dt}$. Repeating the procedure in the proof of Prop. 3.2 (1) for the points $P_{k+1}\overset{\text{def}}{=}(p_P^i,v_P^i)_{k+1}$ with variables defined in Eqs. (21)-(31), the result follows.

3) Since both results (1) and (2) in Prop. 3.2 are solutions to the Eqs. (16)-(17), by combining Eqs. (20) and (27) row by row, such that the determinant of the linear system of equations is not null (whenever $\rho(t,x)>0,\forall t,\forall x\in[0,L]$) as in Eq. (32), the result is also a solution to Eqs. (16)-(17).